

# HORIZONTAL BUOYANCY-DRIVEN FLOW ALONG A DIFFERENTIALLY COOLED UNDERLYING SURFACE

Alan SHAPIRO\*, Evgeni FEDOROVICH\*

\*University of Oklahoma, School of Meteorology, 120 David L. Boren Blvd., Norman, OK 73072, USA

**Summary.** Buoyancy forced flows above cooled surfaces or beneath heated surfaces, commonly encountered in engineering and geophysics, are often horizontal and have a pronounced boundary-layer structure. A combined analytical and numerical analysis of a prototypical flow of this kind induced by a step change in surface cooling is presented. The unsteady governing equations of the problem in the Boussinesq approximation admit solutions that are invariant to a stretching transformation. This property leads to a self-similarity model for the flow variables. The spatial and temporal characteristics of the similarity model solutions are explored and found to be in good agreement with data obtained from high-resolution numerical simulations.

## 1. INTRODUCTION

When a horizontal surface that underlies a quiescent fluid is cooled, diffusion communicates the state of the surface to the fluid, and a statically stable – with respect to vertical displacements – thermal field develops in the fluid. If the magnitude of the cooling varies laterally, buoyancy variations arise within the fluid, and the associated lateral variations in pressure drive a shallow, primarily horizontal current. Following Amin and Riley [1], we refer to such flow types as horizontal free convection. A distinguishing feature of such flows is that buoyancy acts in a direction perpendicular to the principal motion and thus drives the flow only indirectly. In the atmosphere, differential cooling of the underlying surface gives rise to land breezes and other local circulations [2]. Boundary-layer free convective flows along cooled upward-facing horizontal plates or, equivalently, along heated downward-facing plates, reviewed in [3], are of longstanding interest in the engineering heat transfer community.

Very few analyses of the boundary-layer equations have been reported for unsteady horizontal free convection problems. Ingham et al. [4] considered the response of a heated boundary layer to the sudden cooling of a semi-infinite horizontal upward facing plate. The initial flow state satisfied the Stewartson [5] and Gill et al. [6] similarity model for steady flow along a semi-infinite heated upward facing plate. Higuera [7] considered the horizontal convective flow induced by the sudden application of a maintained line heat source at an infinite downward facing surface. Amin and Riley [1] studied the evolution of the boundary layer over an underlying surface whose temperature varied quadratically with the lateral coordinate. If the surface temperature was prescribed to increase away from the plane of symmetry, a steady state could be achieved, but if the surface temperature decreased away from the plane of symmetry, the flow became singular in a finite time.

The present study is concerned with a prototypical class of horizontal free convective flows. Initially quiescent stably stratified fluid fills the half space ( $z > 0$ ) above an infinite horizontal plate at  $z = 0$ . At time  $t = 0$ , a plate cooling (negative buoyancy or negative buoyancy flux) that varies with the lateral coordinate  $x$  is imposed and thereafter maintained. The flux is piecewise constant with a step change at  $x = 0$ . In response to the cooling, a baroclinically-generated circulation develops. The evolving stratification suppresses the vertical branch of this circulation, and the flow has a boundary-layer character typical of motion under conditions of a stable stratification.

## 2. GOVERNING EQUATIONS

We investigate the horizontal free convective flow within a Boussinesq boundary layer framework in which  $x$  derivatives in the stress and diffusion terms are neglected, and the hydrostatic approximation is invoked.

The governing equations of the flow are thus

$$\frac{\partial u}{\partial t} + u \frac{\partial u}{\partial x} + w \frac{\partial u}{\partial z} = -\frac{\partial \pi}{\partial x} + \nu \frac{\partial^2 u}{\partial z^2}, \quad (1)$$

$$0 = -\frac{\partial \pi}{\partial z} + b, \quad (2)$$

$$\frac{\partial b}{\partial t} + u \frac{\partial b}{\partial x} + w \frac{\partial b}{\partial z} = -\gamma w + \kappa \frac{\partial^2 b}{\partial z^2}, \quad (3)$$

$$\frac{\partial u}{\partial x} + \frac{\partial w}{\partial z} = 0. \quad (4)$$

Equations (1) and (2) are the  $x$ - and  $z$ -component equations of motion, (3) is the thermal energy equation and (4) is the incompressibility condition. The normalized pressure perturbation  $\pi \equiv (p - \bar{p})/\rho_r$  is the difference between the pressure  $p$  and the pressure  $\bar{p}(z)$  in a hydrostatic background state normalized by a constant reference density  $\rho_r$ . The buoyancy is defined as  $b \equiv g(\theta - \bar{\theta})/\theta_r$ , where  $\theta$  is temperature (if fluid is a liquid) or potential temperature (if fluid is a gas),  $\theta_r$  is a constant reference value of  $\theta$ ,  $g$  is the acceleration due to gravity, and  $\bar{\theta}(z)$  is the background profile of  $\theta$ . The stratification parameter  $\gamma \equiv (g/\theta_r)d\bar{\theta}/dz$ , kinematic viscosity  $\nu$ , and thermal diffusivity  $\kappa$  are assumed to be constant.

Subtracting the  $x$  derivative of (2) from the  $z$  derivative of (1) and using (4) yields

$$\left( \frac{\partial}{\partial t} + u \frac{\partial}{\partial x} + w \frac{\partial}{\partial z} \right) \frac{\partial u}{\partial z} = -\frac{\partial b}{\partial x} + \nu \frac{\partial^3 u}{\partial z^3}. \quad (5)$$

Introducing the streamfunction  $\psi$ , defined by  $u = \partial\psi/\partial z$ ,  $w = -\partial\psi/\partial x$ , and the non-dimensionalization

$$X \equiv \frac{b_s^{1/3} x}{\nu^{2/3}}, \quad Z \equiv \frac{b_s^{1/3} z}{\nu^{2/3}}, \quad T \equiv \frac{b_s^{2/3} t}{\nu^{1/3}}, \quad B \equiv \frac{b}{b_s}, \quad \Psi \equiv \frac{\psi}{\nu}, \quad \text{Pr} \equiv \frac{\nu}{\kappa}, \quad \Gamma \equiv \frac{\gamma \nu^{2/3}}{b_s^{4/3}}, \quad (6)$$

where  $b_s > 0$  is any convenient buoyancy scale, (4) is automatically satisfied and (3) and (5) become

$$\left( \frac{\partial}{\partial T} + \frac{\partial \Psi}{\partial Z} \frac{\partial}{\partial X} - \frac{\partial \Psi}{\partial X} \frac{\partial}{\partial Z} \right) B = \Gamma \frac{\partial \Psi}{\partial X} + \frac{1}{\text{Pr}} \frac{\partial^2 B}{\partial Z^2}, \quad (7)$$

$$\left( \frac{\partial}{\partial T} + \frac{\partial \Psi}{\partial Z} \frac{\partial}{\partial X} - \frac{\partial \Psi}{\partial X} \frac{\partial}{\partial Z} \right) \frac{\partial^2 \Psi}{\partial Z^2} = -\frac{\partial B}{\partial X} + \frac{\partial^4 \Psi}{\partial Z^4}. \quad (8)$$

Equation (8) is a boundary-layer form of  $Y$ -component vorticity equation with a baroclinic generation term  $\partial B/\partial X$ . Henceforth, when we refer to vorticity we refer to a boundary-layer-approximated form of vorticity  $\partial U/\partial Z = \partial^2 \Psi/\partial Z^2$ , rather than to the full vorticity,  $\partial U/\partial Z - \partial W/\partial X = \nabla^2 \Psi$ .

Far above the surface ( $Z \rightarrow \infty$ ), the vorticity and buoyancy fields are considered to vanish. We do not assume that the velocity components must vanish as  $Z \rightarrow \infty$  but will look to the solution for their behavior. Presumably perturbation pressure gradient forces developing near the leading edge of the low-level current will push parcels upward, out of the way of the advancing flow. In the unstratified fluid case,  $\Gamma = 0$ , a non-zero vertical velocity component  $\partial \Psi/\partial X \neq 0$  that persists as  $Z \rightarrow \infty$  is a legitimate solution of (7) and (8). In the case of stably stratified fluid,  $\Gamma > 0$ , (7) shows that if the buoyancy functions vanish as  $Z \rightarrow \infty$  then the vertical velocity must also vanish as  $Z \rightarrow \infty$ . This is not surprising since stable stratification suppresses vertical motions.

The lower boundary conditions are the impermeability and no-slip conditions, a step-function distribution for  $B$  or  $\partial B/\partial Z$ , and a condition on vorticity to be described below. We anticipate that the baroclinic vorticity production  $\partial B/\partial X$  should vanish at sufficiently large lateral distances from the step change. Accordingly, as  $X \rightarrow \pm\infty$ , the vorticity and velocity components should vanish, all terms in (8) vanish, and (7) reduces to the one-dimensional heat transfer (diffusion) equation. Thus, as  $X \rightarrow \pm\infty$ , the buoyancy can be expressed as a classical solution of the heat equation considered in [9].

Since (7) and (8) comprise a sixth-order system with respect to  $Z$ , the three surface conditions (no-slip, impermeability, and specified buoyancy or buoyancy flux) and two remote conditions (vanishing vorticity and buoyancy) fall one condition short of closing the problem. An appropriate final boundary condition is determined by integrating (2) from the surface up to  $z = \infty$ , where the perturbation pressure is considered to

vanish, obtaining  $\pi(x,0) = -\int_0^{\infty} b(x,z)dz$ . Evaluation of this expression at  $z = 0$  using the impermeability and no-slip conditions yields a lower boundary condition for the normal derivative of vorticity:

$$v \frac{\partial^2 u}{\partial z^2}(x, 0) = -\frac{\partial}{\partial x} \int_0^{\infty} b(x,z)dz.$$

### 3. SIMILARITY MODELS

Application of group-theoretic principles can, in some cases, greatly simplify problems in fluid mechanics, heat transfer, plasma physics and other areas of science and engineering (see, e.g., [10]-[15]). In the group-theoretic approach, analysis of symmetries of the governing partial differential equations yields new dependent and independent variables (special combinations of the original variables, sometimes referred to as similarity variables), in terms of which the equations reduce in dimension. In some cases the original partial differential equations are converted into ordinary differential equations. The simplifications are often more extensive than could be achieved through dimensional analysis alone (i.e., using the Pi Theorem). However, the group-theoretic similarity solutions are only consistent with restricted classes of initial and boundary conditions or governing parameters, and may or may not correspond to physically interesting scenarios. Our focus on horizontal convection flows driven by step-changes in surface buoyancy and buoyancy flux was, in fact, motivated by the outcome of the group analysis.

#### 3.1. Unstratified fluid case

In this section we apply group-theoretic principles to obtain a similarity model for a class of flows that satisfy (7) and (8) for an unstratified fluid ( $\Gamma = 0$ ). Our presentation follows general approach from [12].

Consider the one-parameter family of stretching transformations

$$T' = \mu T, \quad X' = \mu^m X, \quad Z' = \mu^q Z, \quad \Psi' = \mu^r \Psi, \quad B' = \mu^s B, \quad (9)$$

where  $\mu > 0$  is a continuous parameter and  $\mu = 1$  is the identity element. We find that (7) with  $\Gamma = 0$  and (8) are invariant to the transformation (9) provided

$$q = \frac{1}{2}, \quad m = r + \frac{1}{2}, \quad s = 2r - \frac{3}{2}, \quad (10)$$

where  $r$  is arbitrary. Thus, (9) maps any solution  $B = g(X, Z, T)$  and  $\Psi = f(X, Z, T)$  of (7) and (8) to another solution of (7) and (8). We consider the special case for which the solutions themselves are invariant to (9) with exponents (10). By definition, these invariant solutions satisfy  $B' [= \mu^s B = \mu^s g(X, Z, T)] = g(X', Z', T')$  and  $\Psi' [= \mu^r \Psi = \mu^r f(X, Z, T)] = f(X', Z', T')$ , that is

$$\mu^{2r-3/2} g(X, Z, T) = g(\mu^{r+1/2} X, \mu^{1/2} Z, \mu T), \quad (11)$$

$$\mu^r f(X, Z, T) = f(\mu^{r+1/2} X, \mu^{1/2} Z, \mu T). \quad (12)$$

Differentiating (11) and (12) with respect to  $\mu$  and evaluating the results at  $\mu = 1$  leads to the first order linear partial differential equations,

$$\left(2r - \frac{3}{2}\right)g = \left(r + \frac{1}{2}\right)X \frac{\partial g}{\partial X} + \frac{1}{2}Z \frac{\partial g}{\partial Z} + T \frac{\partial g}{\partial T}, \quad (13)$$

$$r f = \left(r + \frac{1}{2}\right)X \frac{\partial f}{\partial X} + \frac{1}{2}Z \frac{\partial f}{\partial Z} + T \frac{\partial f}{\partial T}. \quad (14)$$

The characteristic equations associated with (13) and (14) are

$$\left(2r - \frac{3}{2}\right)^{-1} \frac{dg}{g} = \left(r + \frac{1}{2}\right)^{-1} \frac{dX}{X} = 2 \frac{dZ}{Z} = \frac{dT}{T}, \quad (15)$$

$$\frac{1}{r} \frac{df}{f} = \left(r + \frac{1}{2}\right)^{-1} \frac{dX}{X} = 2 \frac{dZ}{Z} = \frac{dT}{T}. \quad (16)$$

These equations are readily integrated and, denoting  $\sigma \equiv -r - 1/2$ , the general solution is expressed as

$$\Psi = T^{-\sigma-1/2} F(\xi, \eta), \quad B = T^{-2\sigma-5/2} G(\xi, \eta), \quad (17)$$

$$\xi \equiv XT^\sigma, \quad \eta \equiv ZT^{-1/2}, \quad (18)$$

where  $F$  and  $G$  are yet to be determined functions of stretched coordinates  $\xi$  and  $\eta$ . Application of (17) and (18) in (7) and (8) yields

$$\left( -2\sigma - \frac{5}{2} + \sigma\xi \frac{\partial}{\partial\xi} - \frac{1}{2}\eta \frac{\partial}{\partial\eta} + \frac{\partial F}{\partial\eta} \frac{\partial}{\partial\xi} - \frac{\partial F}{\partial\xi} \frac{\partial}{\partial\eta} \right) G = \frac{1}{\text{Pr}} \frac{\partial^2 G}{\partial\eta^2}, \quad (19)$$

$$\left( -\sigma - \frac{3}{2} + \sigma\xi \frac{\partial}{\partial\xi} - \frac{1}{2}\eta \frac{\partial}{\partial\eta} + \frac{\partial F}{\partial\eta} \frac{\partial}{\partial\xi} - \frac{\partial F}{\partial\xi} \frac{\partial}{\partial\eta} \right) \frac{\partial^2 F}{\partial\eta^2} = -\frac{\partial G}{\partial\xi} + \frac{\partial^4 F}{\partial\eta^4}. \quad (20)$$

In proceeding from (7) and (8) to (19) and (20) the number of independent variables has been reduced from three ( $X, Z, T$ ) to two ( $\xi, \eta$ ). In view of (17) and (18), any solutions  $F$  and  $G$  of (19) and (20) deduced as functions of  $\xi$  and  $\eta$  contain all the information needed to infer these solutions at any time.

In terms of the similarity variables, the impermeability and no-slip conditions, and the vorticity boundary condition (see section 2) become, respectively,

$$F(\xi, 0) = 0, \quad \frac{\partial F}{\partial\eta}(\xi, 0) = 0, \quad \frac{\partial^3 F}{\partial\eta^3}(\xi, 0) = -\frac{\partial}{\partial\xi} \int_0^\infty G(\xi, \eta) d\eta. \quad (21)$$

We assume the vorticity and buoyancy vanish far above the surface (as  $Z \rightarrow \infty$ ) and are zero initially everywhere above the plate (as  $T \rightarrow 0$  for  $Z > 0$ ). Since  $Z \rightarrow \infty$  and  $T \rightarrow 0$  (for  $Z > 0$ ) are both associated with  $\eta \rightarrow \infty$ , these two conditions reduce to a single condition:

$$\frac{\partial^2 F}{\partial\eta^2}, G \rightarrow 0 \quad \text{as} \quad \eta \rightarrow \infty. \quad (22)$$

Such a conflation of boundary and initial conditions is typical of similarity models.

The type of the lower boundary condition on the buoyancy (or buoyancy flux) functions will be fixed by the choice of  $\sigma$ . In the following analyses we seek values of  $\sigma$  consistent with buoyancy or buoyancy flux functions that are (i) steady-state and (ii) vary as piecewise constant distributions with step changes at  $X = 0$  ( $\xi = 0$ ).

We first consider a step change in the **surface buoyancy** which is suddenly imposed at  $T = 0$  and maintained thereafter.

To obtain a surface buoyancy function  $B(X, 0) = T^{-2\sigma-5/2} G(\xi, 0)$  that is in a steady state (for  $T > 0$ ), the time dependence in  $G(\xi, 0)$  must be such that it cancels the  $T^{-2\sigma-5/2}$  factor in front of it. This constrains the surface buoyancy functions to the form:

$$G(\xi, 0) = C\xi^{2+5/(2\sigma)}, \quad B(X, 0) = CX^{2+5/(2\sigma)}, \quad (23)$$

where  $C$  is constant or piecewise constant with a step change at  $X = 0$  ( $\xi = 0$ ). For  $B(X, 0)$  to be piecewise constant,  $C$  must be a piecewise constant and thus  $\sigma = -5/4$ . In this case, (17)-(20) become

$$\Psi = T^{3/4} F(\xi, \eta), \quad B = G(\xi, \eta), \quad (24)$$

$$\xi \equiv XT^{-5/4}, \quad \eta \equiv ZT^{-1/2}, \quad (25)$$

$$\left( -\frac{5}{4}\xi \frac{\partial}{\partial\xi} - \frac{1}{2}\eta \frac{\partial}{\partial\eta} + \frac{\partial F}{\partial\eta} \frac{\partial}{\partial\xi} - \frac{\partial F}{\partial\xi} \frac{\partial}{\partial\eta} \right) G = \frac{1}{\text{Pr}} \frac{\partial^2 G}{\partial\eta^2}, \quad (26)$$

$$\left( -\frac{1}{4} - \frac{5}{4}\xi \frac{\partial}{\partial\xi} - \frac{1}{2}\eta \frac{\partial}{\partial\eta} + \frac{\partial F}{\partial\eta} \frac{\partial}{\partial\xi} - \frac{\partial F}{\partial\xi} \frac{\partial}{\partial\eta} \right) \frac{\partial^2 F}{\partial\eta^2} = -\frac{\partial G}{\partial\xi} + \frac{\partial^4 F}{\partial\eta^4}. \quad (27)$$

In view of (24) and (25),  $B$  is invariant along curves defined by constant values of  $\xi$  and  $\eta$ . The values of  $B$  corresponding to the constants  $\xi = \xi_c$  and  $\eta = \eta_c$  propagate in  $(X, Z)$  at speeds

$$\frac{dX}{dT} = \frac{5}{4}\xi_c T^{1/4}, \quad (X \sim T^{5/4}), \quad \frac{dZ}{dT} = \frac{1}{2}\eta_c T^{-1/2}, \quad (Z \sim T^{1/2}). \quad (28)$$

Thus, the vertical propagation speed decreases with time, while the horizontal propagation speed increases with time (albeit slowly, as one-quarter power of  $T$ ), except along the vertical axis ( $X = 0$ ) where the horizontal propagation speed is zero. The paths traced out over time by values of constant  $B$  radiate outward

as  $Z \propto X^{2/5}$ , with the exception of the paths that originate on the vertical axis, which are given by  $X = 0$ ,  $Z \propto T^{1/2}$ . An analogously straightforward evaluation of the propagation speeds of the velocity components is not possible. However, in view of (24) and (25) it is easy to show that any local extremum or inflection point (with respect to  $X$  and/or  $Z$ ) in any of the velocity components or buoyancy functions propagate according to (28).

Now we consider a piecewise constant *surface buoyancy flux*  $\partial B / \partial Z(X, 0) = T^{-2\sigma-3} \partial G / \partial \eta(\xi, 0)$  with a step change at  $X = 0$  ( $\xi = 0$ ).

According to (17) and (18), if the flux in the steady state, then

$$\frac{\partial G}{\partial \eta}(\xi, 0) = D \xi^{2+3/\sigma}, \quad \frac{\partial B}{\partial Z}(X, 0) = D X^{2+3/\sigma}. \quad (29)$$

where  $D$  is constant or piecewise constant with step change at  $X = 0$  ( $\xi = 0$ ). In order for the flux to be piecewise constant,  $D$  must be piecewise constant and hence  $\sigma = -3/2$ . In this case, (17)-(20) become

$$\Psi = T F(\xi, \eta), \quad B = T^{1/2} G(\xi, \eta), \quad (30)$$

$$\xi \equiv X T^{-3/2}, \quad \eta \equiv Z T^{-1/2}, \quad (31)$$

$$\left( \frac{1}{2} - \frac{3}{2} \xi \frac{\partial}{\partial \xi} - \frac{1}{2} \eta \frac{\partial}{\partial \eta} + \frac{\partial F}{\partial \eta} \frac{\partial}{\partial \xi} - \frac{\partial F}{\partial \xi} \frac{\partial}{\partial \eta} \right) G = \frac{1}{\text{Pr}} \frac{\partial^2 G}{\partial \eta^2}, \quad (32)$$

$$\left( -\frac{3}{2} \xi \frac{\partial}{\partial \xi} - \frac{1}{2} \eta \frac{\partial}{\partial \eta} + \frac{\partial F}{\partial \eta} \frac{\partial}{\partial \xi} - \frac{\partial F}{\partial \xi} \frac{\partial}{\partial \eta} \right) \frac{\partial^2 F}{\partial \eta^2} = -\frac{\partial G_n}{\partial \xi} + \frac{\partial^4 F}{\partial \eta^4}. \quad (33)$$

It follows from (30) and (31) that the vertical gradients  $\partial B / \partial Z$  are invariant along curves defined by constant values of  $\xi$  and  $\eta$ . The value of  $\partial B / \partial Z$  corresponding to the constants  $\xi = \xi_c$  and  $\eta = \eta_c$  propagates at speeds

$$\frac{dX}{dT} = \frac{3}{2} \xi_c T^{1/2}, \quad (X \sim T^{3/2}), \quad \frac{dZ}{dT} = \frac{1}{2} \eta_c T^{-1/2}, \quad (Z \sim T^{1/2}). \quad (34)$$

Thus, the vertical propagation speed decreases with time, while the horizontal propagation speed increases with time as one-half power of  $T$ , except along the vertical axis where the horizontal propagation speed is zero. The paths traced out over time by values of constant  $\partial B / \partial Z$  radiate outward as  $Z \propto X^{1/3}$ , with the exception of the paths that originate on the vertical axis, which are given by  $X = 0$ ,  $Z \propto T^{1/2}$ . It also follows from (30) and (31) that the vorticity  $\partial^2 \Psi / \partial Z^2$  is invariant along curves defined by constant values of  $\xi$  and  $\eta$ . Therefore, the pattern of vorticity propagates in the same manner as the pattern of vertical buoyancy gradient. The patterns themselves, however, as solutions of (32) and (33), are expected to be different. It is easy to show that (34) also applies to the propagation of any local extremum or inflection point in any of the velocity components or buoyancy functions.

### 3.2. Stratified fluid case

In this case of  $\Gamma > 0$ , (7) and (8) are invariant to the stretching transformation (9) provided the transformation exponents satisfy (10) and the additional constraint  $m = r + 1 - s$ . Thus, the exponents are

$$q = \frac{1}{2}, \quad m = \frac{3}{2}, \quad s = \frac{1}{2}, \quad r = 1 \quad (\sigma = -3/2). \quad (35)$$

Note that there is no arbitrary element in the exponents as there was in (10) for the unstratified fluid case. In the stably stratified case, the similarity scalings are thus of the form:

$$\Psi = T F(\xi, \eta), \quad B = T^{1/2} G(\xi, \eta). \quad (36)$$

$$\xi \equiv X T^{-3/2}, \quad \eta \equiv Z T^{-1/2}. \quad (37)$$

The above scalings are identical to the scalings (30) and (31) that apply to a step change in the surface buoyancy flux in an unstratified fluid. Thus, for the case of stable stratification, the appropriate boundary condition is a flux condition and there is no provision for a step change in surface buoyancy within the context of this similarity model. Since (36), (37) are identical to (30), (31), the propagation of any local extremum or inflection point in any of the velocity components or buoyancy functions in the stably stratified

case is described by (34).

Application of (36) and (37) in (7) and (8) yields

$$\left( \frac{1}{2} - \frac{3}{2} \xi \frac{\partial}{\partial \xi} - \frac{1}{2} \eta \frac{\partial}{\partial \eta} + \frac{\partial F}{\partial \eta} \frac{\partial}{\partial \xi} - \frac{\partial F}{\partial \xi} \frac{\partial}{\partial \eta} \right) G = \Gamma \frac{\partial F}{\partial \xi} + \frac{1}{\text{Pr}} \frac{\partial^2 G}{\partial \eta^2}, \quad (38)$$

$$\left( -\frac{3}{2} \xi \frac{\partial}{\partial \xi} - \frac{1}{2} \eta \frac{\partial}{\partial \eta} + \frac{\partial F}{\partial \eta} \frac{\partial}{\partial \xi} - \frac{\partial F}{\partial \xi} \frac{\partial}{\partial \eta} \right) \frac{\partial^2 F}{\partial \eta^2} = -\frac{\partial G}{\partial \xi} + \frac{\partial^4 F}{\partial \eta^4}. \quad (39)$$

#### 4. VALIDATION OF SIMILARITY MODELS

In view of (6), (24), and (25), the similarity scalings for the dimensional velocity and buoyancy fields in the case of a step change of surface buoyancy can be written as

$$u = b_s^{1/2} \nu^{1/4} t^{1/4} \frac{\partial F}{\partial \eta}, \quad w = -\sqrt{\frac{\nu}{t}} \frac{\partial F}{\partial \xi}, \quad b = b_s G(\xi, \eta). \quad (40)$$

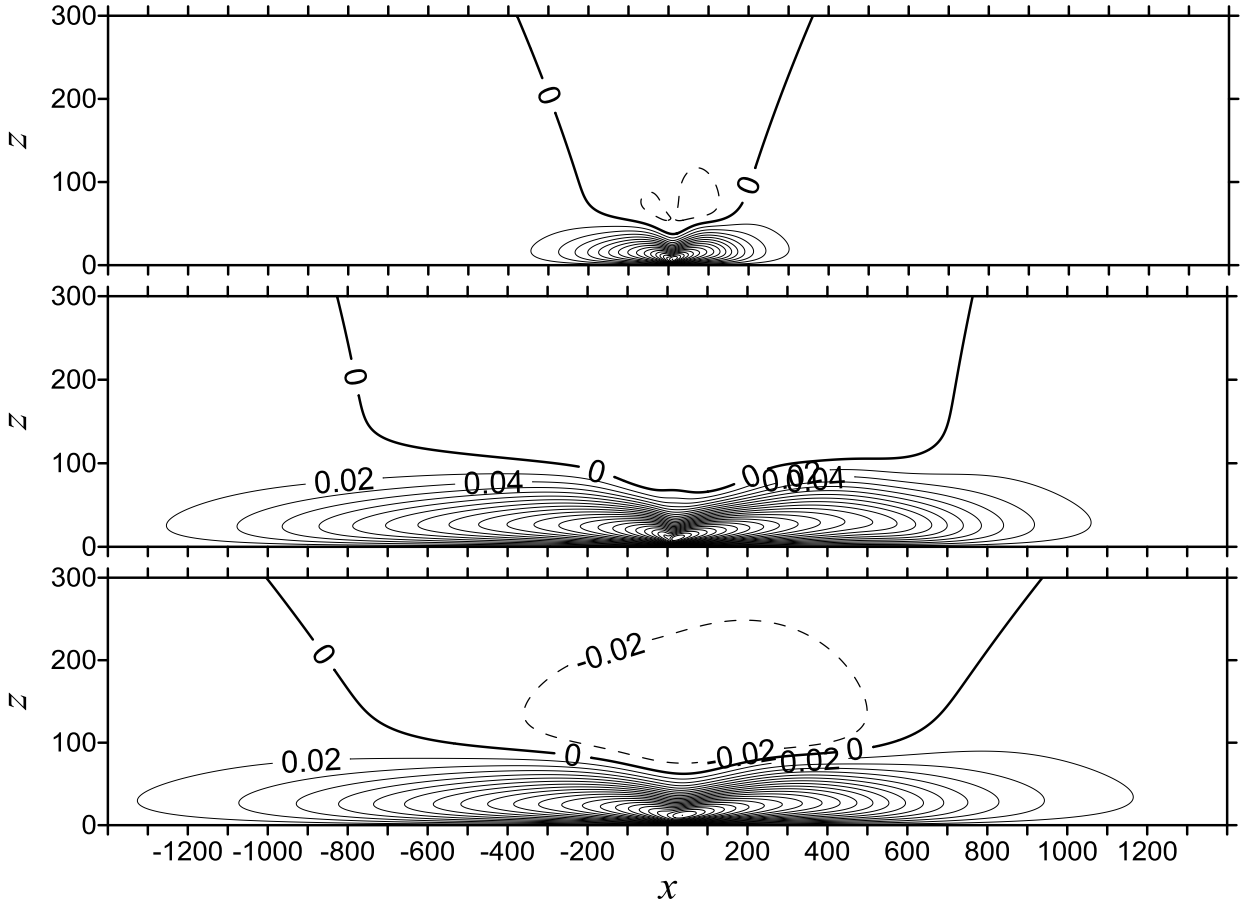


Fig. 1. Vertical cross-sections of  $u$  ( $\text{m s}^{-1}$ ) for the flow case with surface buoyancy forcing and unstratified fluid. Shown are numerically simulated  $u$  at  $t_0 = 326$  s (top) and  $t_1 = 905$  s (middle), and the similarity-model extended  $u$  at  $t_1 = 905$  s (bottom). The isoline interval is  $0.02 \text{ m s}^{-1}$ .

On the other hand, in the case of a step change of surface buoyancy flux, (6), (30), and (31) provide the following dimensional variable scalings:

$$u = b_s^{2/3} \nu^{1/6} t^{1/2} \frac{\partial F}{\partial \eta}, \quad w = -\sqrt{\frac{\nu}{t}} \frac{\partial F}{\partial \xi}, \quad b = \frac{b_s^{4/3} t^{1/2}}{\nu^{1/6}} G(\xi, \eta). \quad (41)$$

The above scalings were validated against data from numerical simulations using the Boussinesq equations of motion, thermodynamic energy, and mass conservation solved for the same flow cases that have been investigated with similarity model, but without boundary layer or hydrostatic approximations.

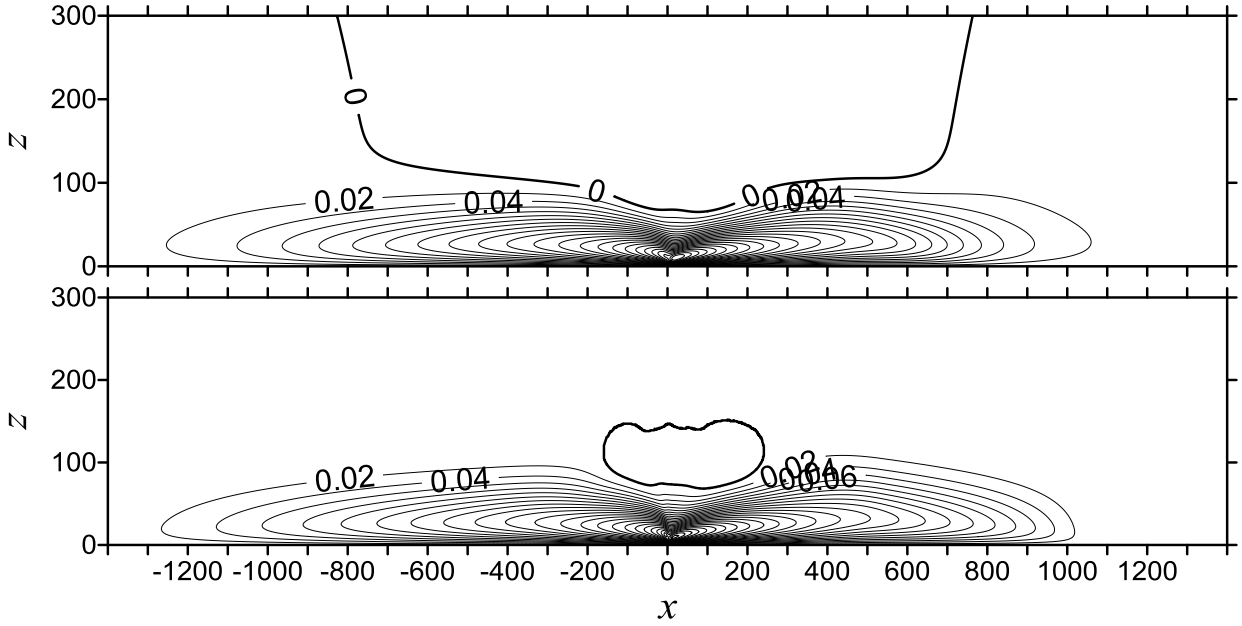


Fig. 2. Horizontal flow component  $u$  ( $\text{m s}^{-1}$ ) in the flow case with surface buoyancy forcing and unstratified fluid. Numerically simulated  $u$  at  $t_1 = 905$  s (top) is compared with similarity-model prediction of  $u$  at  $t_1 = 905$  s (bottom). The isoline interval is  $0.02 \text{ m s}^{-1}$ .

The numerical procedures used herein are patterned on the work of Fedorovich et al. [16] and were previously employed in the studies of natural-convection and slope flows of Shapiro and Fedorovich ([17]-[19]), Fedorovich and Shapiro ([20],[21]) and Burkholder et al. [22]. The numerically solved equations are the Boussinesq equations of motion for a non-rotating viscous fluid, the thermodynamic energy, and the standard elliptic equation for the perturbation pressure that results from taking the divergence of the equations of motion and applying the mass conservation equation under conditions of incompressibility. The model equations are discretized on a staggered, Cartesian grid with a uniform spacing ( $\Delta x = \Delta y = \Delta z$ ) in a rectangular box-like domain. The spatial derivatives are discretized with second-order finite difference expressions. The prognostic variables are integrated using a leapfrog scheme with a weak Asselin filter. The elliptic equation for the perturbation pressure is solved at each time step using a Fast Fourier Transform technique over horizontal planes, and a tri-diagonal matrix inversion in the vertical direction. On the surface, no-slip and impermeability conditions are imposed, the surface buoyancy (or buoyancy flux) is prescribed, and the vertical derivative of the perturbation pressure is calculated as a residual from the vertical component of the equation of motion. At the top of the computational domain, the normal gradients of all variables are set to zero. Periodic boundary conditions are imposed for all variables on the four lateral boundaries. To simulate a flow that is independent of the  $y$ -coordinate using a three-dimensional code, it suffices to allocate only four grid points in the  $y$  direction.

First we show results for the natural convection flow generated by an imposed piecewise surface buoyancy in an unstratified fluid. For the validation experiment, the numerical simulation was run with  $\Delta x = \Delta y = \Delta z = 1 \text{ m}$ ,  $b_s = -0.2 \text{ m s}^{-2}$  at  $x \leq 0$ ,  $b_s = -0.1 \text{ m s}^{-2}$  at  $x > 0$ , and  $\nu = \kappa = 1 \text{ m}^2 \text{ s}^{-1}$  ( $\text{Pr} = 1$ ). Numerical data at  $t_0 = 326$  s were used in the similarity relationships (40) to evaluate  $\partial F/\partial \eta$ ,  $\partial F/\partial \xi$ , and  $G$  functions, which were then employed back in (40) to extend flow fields to a later time  $t_1 = 905$  s. In Fig. 1, the similarity-model extended  $u$  field is compared with the numerically simulated  $u$  at  $t_1$ . A good agreement between the numerically simulated and similarity-extended fields is evident.

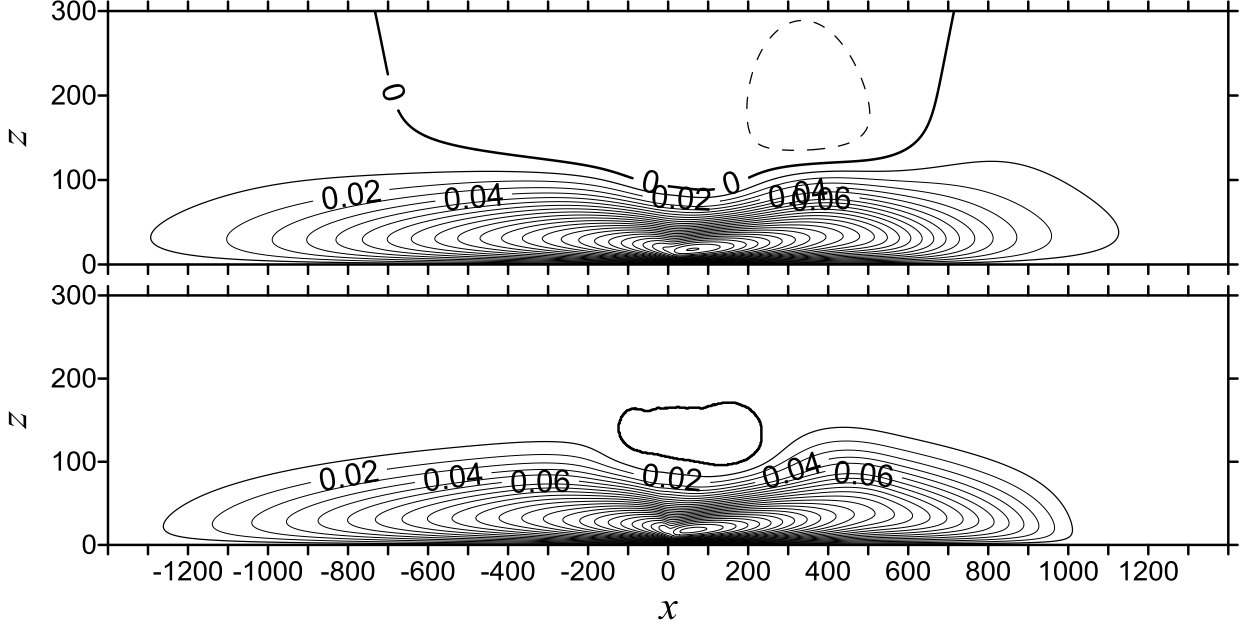


Fig. 3. Horizontal flow component  $u$  ( $\text{m s}^{-1}$ ) in the flow case with surface buoyancy flux forcing and unstratified fluid. Numerically simulated  $u$  at  $t_1 = 1612$  s (top) is compared with similarity-model prediction of  $u$  at  $t_1 = 1612$  s (bottom). The isoline interval is  $0.02 \text{ m s}^{-1}$ .

Another way to validate the similarity model would be to directly compare the similarity theory prediction for a specific flow field at a particular time with the numerical prediction for the same time. In this case, equations (26) and (27) of the similarity model have been solved numerically with respect to  $F$  and  $G$ , and the resulting flow fields at given  $t$  have been evaluated against numerically simulated flow fields using similarity relationships (40). The results of such a comparison for  $u$  in the case with surface buoyancy forcing are illustrated in Fig. 2. The similarity model in this case rather accurately predicts minima and maxima of the  $u$  field, providing  $u_{\min} = -0.013 \text{ m s}^{-1}$  and  $u_{\max} = 0.49 \text{ m s}^{-1}$  as compared to  $u_{\min} = -0.020 \text{ m s}^{-1}$  and  $u_{\max} = 0.48 \text{ m s}^{-1}$  predicted by the numerical model.

Similarity model predictions for the horizontal flow component in the cases with surface buoyancy flux forcing are compared to numerical simulation data in Figs. 3 and 4 for the cases of unstratified and stratified fluid, respectively.

In Fig. 3, the  $u$  field, evaluated at  $t_1 = 1612$  s using the similarity-model equations (32) and (33) for the case of an unstratified fluid together with the first of the similarity scaling relationships (41), is compared to its numerically simulated counterpart at the same  $t_1$ . The numerical simulation for this case was run with  $\Delta x = \Delta y = \Delta z = 1 \text{ m}$ ,  $db/dz|_s = 0.002 \text{ s}^{-2}$  at  $x \leq 0$ ,  $db/dz|_s = 0.001 \text{ s}^{-2}$  at  $x > 0$ , and  $\nu = \kappa = 1 \text{ m}^2 \text{ s}^{-1}$  ( $\text{Pr} = 1$ ). The similarity model predicts  $u_{\min} = -0.005 \text{ m s}^{-1}$  and  $u_{\max} = 0.25 \text{ m s}^{-1}$ , while the numerical simulation provides  $u_{\min} = -0.015 \text{ m s}^{-1}$  and  $u_{\max} = 0.25 \text{ m s}^{-1}$ , i.e. the maximum velocity value is captured extremely well by the similarity model.

In Fig. 4, the  $u$  field, evaluated at  $t_1 = 994$  s using the similarity-model equations (38) and (39) for the case of a stratified fluid together with the first of the similarity scaling relationships (41), is compared to the numerically simulated  $u$  at the same  $t_1$ . The parameters of the numerical simulation for this case are:  $\Delta x = \Delta y = \Delta z = 1 \text{ m}$ ,  $db/dz|_s = 0.002 \text{ s}^{-2}$  at  $x \leq 0$ ,  $db/dz|_s = 0.001 \text{ s}^{-2}$  at  $x > 0$ ,  $\gamma = 0.001 \text{ s}^{-2}$ , and  $\nu = \kappa = 1 \text{ m}^2 \text{ s}^{-1}$  ( $\text{Pr} = 1$ ). The similarity model predicts  $u_{\min} = -0.030 \text{ m s}^{-1}$  and  $u_{\max} = 0.12 \text{ m s}^{-1}$ , while the numerical simulation yields  $u_{\min} = -0.028 \text{ m s}^{-1}$  and  $u_{\max} = 0.13 \text{ m s}^{-1}$ , so the similarity model predictions are again in a good agreement with the numerical simulation results.

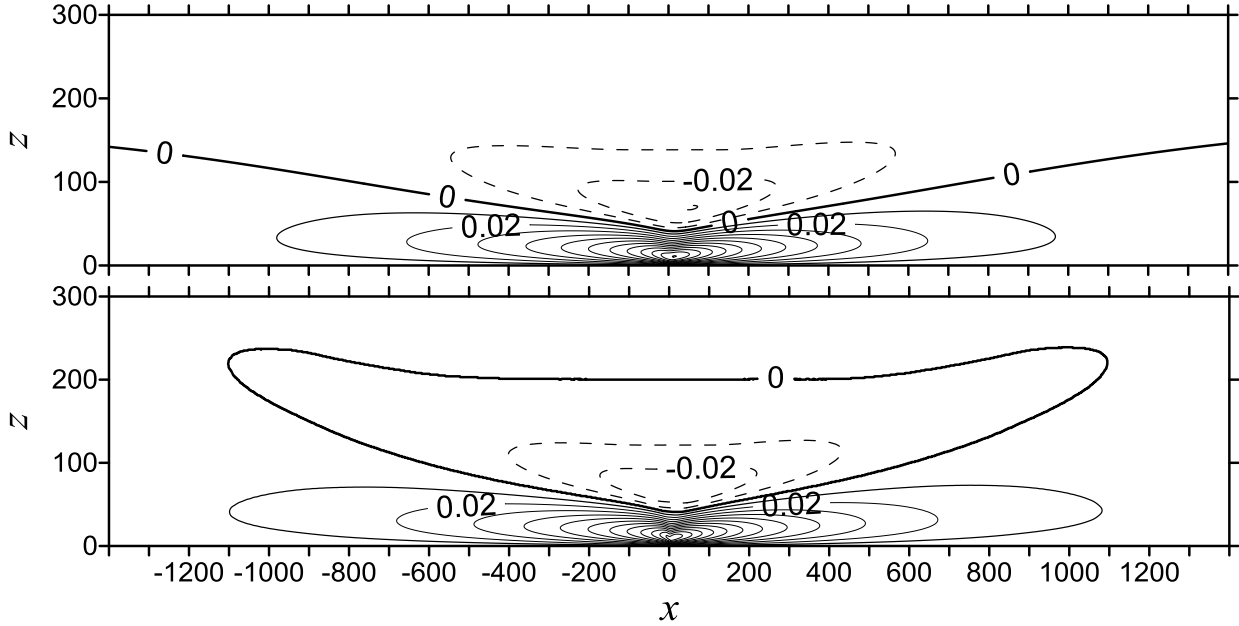


Fig. 4. Horizontal flow component  $u$  ( $\text{m s}^{-1}$ ) in the flow case with surface buoyancy flux forcing and stratified fluid ( $\gamma = 0.001 \text{ s}^{-2}$ ). Numerically simulated  $u$  at  $t_1 = 994 \text{ s}$  (top) is compared with similarity-model prediction of  $u$  at  $t_1 = 994 \text{ s}$  (bottom). The isoline interval is  $0.02 \text{ m s}^{-1}$ .

## 5. CONCLUDING REMARKS

We have presented a combined analytical and numerical investigation of a class of unsteady horizontal free convection flows induced by different types of suddenly imposed laterally varying surface cooling. Similarity models were obtained by exploiting the invariance of the governing equations – boundary layer versions of the Boussinesq equations of motion, energy and mass conservation – to a simple stretching transformation. Models were developed for flows of unstratified fluids driven by a suddenly imposed step change (with respect to lateral coordinate) in surface buoyancy and surface buoyancy flux, and for flows of stably stratified fluids driven by a step change in surface buoyancy flux. The investigated flows were characterized by a predominantly horizontal current with a peak horizontal velocity component that increased weakly with time: as  $t^{1/4}$  for the flow caused by a step change in buoyancy in the unstratified fluid and as  $t^{1/2}$  for the flow driven by a step change in surface buoyancy flux (regardless of stratification). The boundary-layer depth increased as  $t^{1/2}$ , indicating rapid initial growth (once the boundary-layer regime was achieved) followed by a subsequent gradual reduction of the growth rate. The validity of the similarity models was confirmed by comparing similarity predictions to data from numerical simulations in which boundary-layer approximations were not imposed.

If the governing equations are extended to include the Coriolis force, non-hydrostatic terms or lateral stress or diffusion terms, they are no longer invariant to the stretching transformation, and similarity models (if they exist) are not apparent. On the other hand, it can be shown that our similarity framework easily extends to horizontal convection flows of multi-component fluids due to step-changes in surface concentration (for stratified or unstratified fluids) or surface concentration flux (for unstratified fluids).

## REFERENCES

- [1] Amin, N., Riley, N. Horizontal free convection. Proc. R. Soc. Lond. A 427:371-384, 1990.
- [2] Simpson, J. E. Sea breeze and local wind. Cambridge University Press, 1994.

- [3] Gebhart, B., Jaluria, Y., Mahajan, R. L., Sammakia, B. Buoyancy-induced flows and transport. New York, Hemisphere Publishing Corporation, 1988.
- [4] Ingham, D. B., Merkin, J. H., Pop, I. Flow past a suddenly cooled horizontal plate. *Wärme- und Stoffübertragung* 20:237-241, 1986.
- [5] Stewartson, K. On the free convection from a horizontal plate. *Z. Angew. Math. Phys.* 9:276-282, 1958.
- [6] Gill, W. N., Zeh, D. W., del Casal, E. Free convection on a horizontal plate. *Z. Angew. Math. Phys.* 16:539-541, 1965.
- [7] Higuera, F. J. Natural convection flow due to a heat source under an infinite horizontal surface. *Phys. Fluids* 10:3014-3016, 1998.
- [8] Bluman, G. W., Cole, J. D. Similarity methods for differential equations. Springer-Verlag, 1974.
- [9] Carslaw, H. S., Jaeger, J. C. Conduction of heat in solids. 2nd edition, Oxford University Press, 1959.
- [10] Birkhoff, G. *Hydrodynamics: a study in logic, fact and similitude*. New York, Dover, 1955.
- [11] Bluman, G. W., Cole, J. D. Similarity methods for differential equations. New York, Springer-Verlag, 1974.
- [12] Dresner, L. Similarity solutions of nonlinear partial differential equations. London, Pitman Books, 1983.
- [13] Hill, J. M. Differential equations and group methods for scientists and engineers. Boca Raton, Florida, CRC Press, 1992.
- [14] Ibragimov, N. H. (Ed.) CRC handbook of Lie group analysis of differential equations, Vol. I: Symmetries, exact solutions, and conservation laws. Boca Raton, Florida, CRC Press, 1994.
- [15] Ibragimov, N. H. (Ed.) CRC handbook of Lie group analysis of differential equations, Vol. II: Applications in engineering and physical sciences. Boca Raton, Florida, CRC Press, 1995.
- [16] Fedorovich, E., Nieuwstadt, F. T. M., Kaiser, R. Numerical and laboratory study of a horizontally evolving convective boundary layer. Part I: Transition regimes and development of the mixed layer. *J. Atmos. Sci.* 58:70-86, 2001
- [17] Shapiro, A., Fedorovich, E. Prandtl number dependence of unsteady natural convection along a vertical plate in a stably stratified fluid. *Int. J. Heat Mass Transfer* 47:4911–4927, 2004.
- [18] Shapiro, A., Fedorovich, E. Natural convection in a stably stratified fluid along vertical plates and cylinders with temporally-periodic surface temperature variations. *J. Fluid Mech.* 546:295-311, 2006.
- [19] Shapiro, A., Fedorovich, E. Coriolis effects in homogeneous and inhomogeneous katabatic flows. *Q. J. Roy. Meteorol. Soc.* 134:353-370, 2008.
- [20] Fedorovich, E., Shapiro, A. Structure of numerically simulated katabatic and anabatic flows along steep slopes. *Acta. Geophys.* 57:981-1010, 2009.
- [21] Fedorovich, E., Shapiro, A. Turbulent natural convection along a vertical plate immersed in a stably stratified fluid. *J. Fluid. Mech.* 636:41-57, 2009.
- [22] Burkholder, B., Shapiro A., Fedorovich, E. Katabatic flow induced by a cross-slope band of surface cooling. *Acta. Geophys.* 57:923-949, 2009.